Spin coherence generation in negatively charged self-assembled (In,Ga)As quantum dots by pumping excited trion states

A. B. Henriques,[1] A. Schwan,[2] S. Varwig,[2] A. D. B. Maia,[1] A. A. Quivy,[1] D. R. Yakovlev,[2] and M. Bayer[2]
[1]*Instituto de Fisica, Universidade de Sao Paulo, 05315-970 Sao Paulo, Brazil*
[2]*Experimentelle Physik II, Technische Universität Dortmund, D-44221 Dortmund, Germany*
(Received 23 July 2012; revised manuscript received 7 September 2012; published 28 September 2012)

Spin coherence generation in an ensemble of negatively charged (In,Ga)As/GaAs quantum dots was investigated by picosecond time-resolved pump-probe spectroscopy measuring ellipticity. Robust coherence of the ground-state electron spins is generated by pumping excited charged exciton (trion) states. The phase of the coherent state, as evidenced by the spin ensemble precession about an external magnetic field, varies relative to spin coherence generation resonant with the ground state. The phase variation depends on the pump photon energy. It is determined by (a) pumping dominantly either singlet or triplet excited states, leading to a phase inversion, and (b) the subsequent carrier relaxation into the ground states. From the dependence of the precession phase and the measured g factors, information about the quantum dot shell splitting and the exchange energy splitting between triplet and singlet states can be extracted in the ensemble.

DOI: 10.1103/PhysRevB.86.115333 PACS number(s): 78.20.−e

I. INTRODUCTION

The spin of an electron confined in a quantum dot (QD) offers the opportunity to store and manipulate phase coherence over much longer time scales than it is typically possible in charge based devices. Thanks to the spin orbit interaction, spin can be accessed through the electric fields of lasers exciting the orbital levels of an electron, which facilitates the optical orientation mechanism.[1] An all-optical implementation of spin control is of particular interest, since it takes full advantage of modern laser technology to achieve ultrafast schemes of quantum information processing. Various problems related to the spin coherence of carriers confined in QDs have been already addressed in single-QD studies during the past decade. These efforts have concerned initialization,[2–6] decoherence,[7] and manipulation[8–13] of spins, stimulated by the diVincenzo criteria[14] that have to be fulfilled for quantum information implementations.

These topics have also directed studies of electron spin coherence in *ensembles* of negatively charged QDs.[15] It was shown that circularly polarized light pulses resonant with the QD energy gap leads to spin coherence generation.[16] When free motion of an electron is hindered and the electron is localized within a QD, its spin relaxation is highly suppressed[17,18] as a result of which the coherence of a QD electron spin can last much longer than in a bulk material. The coherence time of an electron spin in negatively charged (In,Ga)As/GaAs QDs was found to be $T_2 = 3\ \mu$s,[19] which is orders of magnitude greater than in bulk GaAs.[20] Such long spin coherence times make charged QDs interesting candidates for quantum information processing devices, which demand coherent manipulation to be performed during times much shorter than the coherence time. Further, it was already demonstrated that the electron spins in a negatively charged QD ensemble can be arbitrarily rotated on the picosecond time scale by optical pumping in the vicinity of the trion resonance.[21]

In this work, we shall demonstrate ground-state spin coherence generation in (In,Ga)As/GaAs QDs when the photon energy of the pumping light is scanned from the QD ground state to the first excited-state transition. Depending on the spin structure of the trion in the excited shell, the phase of the spin oscillations can be initialized either in the "up" or "down" state. From the dependence of the measured g factor on photon energy, information about the shell splitting can be derived which can otherwise not be accessed by linear optics on the strongly inhomogeneously broadened ensemble.

Spin coherence generation for nonresonant excitation is also of high interest because doing so laser stray light can be suppressed, when testing the coherence by the probe beam. Recently, further perspectives have been opened for nonresonant excitation of a single QD.[22] In these studies it was shown that nonresonant excitation could be used for optical gating: a single QD could be switched on and off for coherently driving the ground-state transition using a weak laser with photon energy as far away from resonance as the gap of the barrier material surrounding the QD.

II. EXPERIMENTAL

The structure investigated contained (In,Ga)As/GaAs self-assembled QDs, modulation-doped to obtain an average occupation of one electron per dot. The sample was grown by molecular beam epitaxy on a [100]-oriented GaAs substrate. The sample contained 10 layers of (In,Ga)As QDs, separated by wide GaAs barriers, and Si δ-doping sheets 15 nm above and below each QD layer. The sample was thermally annealed for 30 s at 950°C, so its photoluminescence (PL) emission occurs around 1.37 eV. The sample was investigated using a magneto-optical cryostat with the temperature fixed at $T = 6$ K. For pump-probe time-resolved ellipticity (TRE) measurements, a magnetic field of 1.5 T was applied in the Voigt geometry.

This field strength was chosen to have, on the one hand, fast enough spin precession, while, on the other hand, being not too strongly affected by spin dephasing. A Ti-sapphire laser emitting pulses with a duration of ∼1 ps [∼2 meV full width at half maximum (FWHM)] at 75.6-MHz repetition rate was used. The ellipticity of the linearly polarized probe pulse was measured using a standard technique based on

phase-sensitive balanced detection.[23] The ellipticity signal detected is associated with a large number of simultaneously excited QDs. The number of QDs contributing to the signal can be estimated in the following way. The dot density in the sample investigated is 4.0×10^{10} cm^{-2}.[24] The probe beam was focused into a spot on the sample of diameter $\sim$50 μm, which corresponds to the illumination of 10 million dots in the 10-layer sample, about 50% of which we assume are either neutral or multiply charged, and the remaining QDs are singly negatively charged. In the latter QDs only a small fraction will be resonant with the pump beam. Using the PL spectrum (full width at half maximum 30 meV) as a measure of the band-gap distribution in the QD ensemble, and taking the excitation photon energy uncertainty to be 2 meV, only 1/15 of the total number of illuminated QDs will be excited. Thus, the estimated number of QDs that contribute to the ellipticity signal is estimated to be of the order of a few hundred thousand.

III. RESULTS AND DISCUSSION

Figure 1 shows the photoluminescence (PL) of the sample, taken at $T = 6$ K, for an excitation energy of 1.55 eV, well above the GaAs barrier of the QDs. The PL has a maximum at 1.370 eV with a FWHM of 30 meV. For photon energies greater than the QD barrier, assuming that the photoexcited electron-hole pairs are captured stochastically into any of the QDs of the ensemble with equal probability,[25] the PL profile will reflect the energy gap distribution of the QD ensemble. The 30 meV FWHM value of the PL, which is quite large for annealed QDs, is explained by the relatively small size of the dots. Atomic force microscopy done on a sample grown under identical conditions showed that before annealing the dots have a base of 20 nm and a height of 5 nm.[24] Therefore, fluctuations in size parameters in the dot ensemble lead to a stronger variation in the optical transition energies than in a QD sample with larger dots, as shown in Ref. 24. The PL spectrum shown in Fig. 1 was taken at an excitation power density of 4 W/cm^2, but increasing the excitation density did not lead to a well separated p- and d-shell emission as observed for a

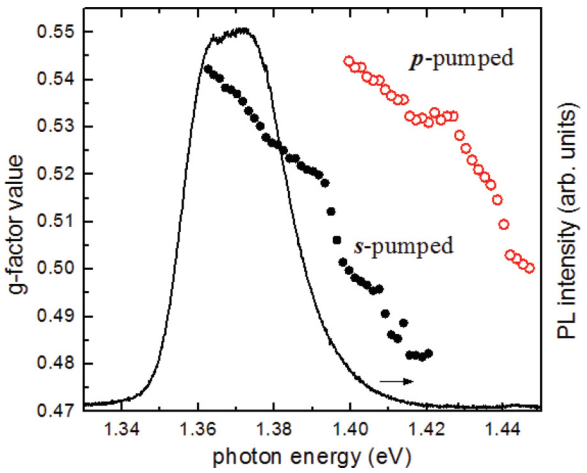

FIG. 1. (Color online) Photoluminescence taken at $T = 6$ K for 1.55-eV excitation photon energy and excitation power density of 4 W/cm^2. Symbols represent absolute values of the electron g factor extracted from the TRE oscillations vs. pump-probe photon energy.

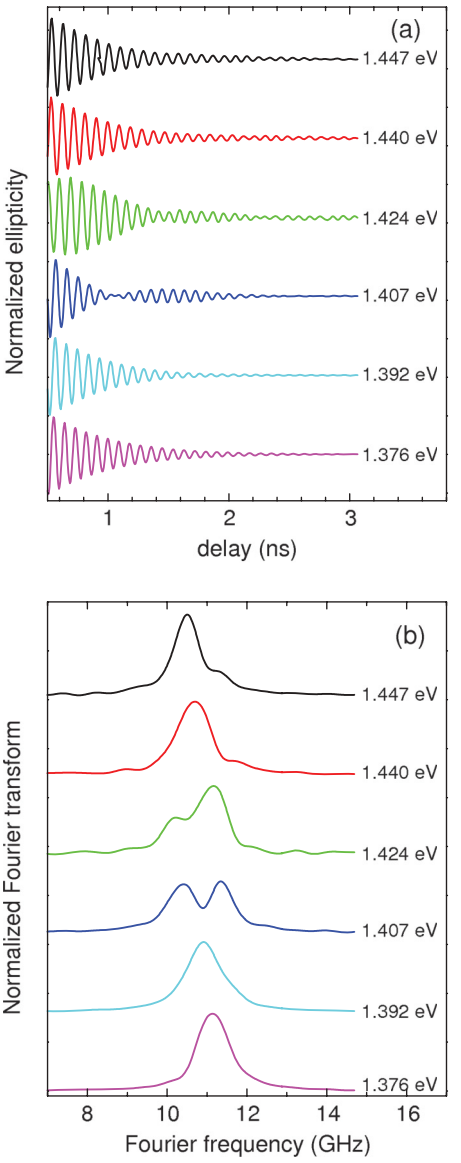

FIG. 2. (Color online) (a) TRE as function of the delay between the pump and probe pulses at $B = 1.5$ T. $T = 6$ K. The energy of the pump/probe photons for each curve is shown. (b) Fourier transform of the TRE oscillations shown in panel (a).

similar QD sample,[26] which is attributed to the inhomogeneous broadening.

Figure 2(a) shows the TRE curves for different pump photon energies. The photon energies chosen ranged from the low energy flank of the QD photoluminescence to energies resonant with excited QD states. The TRE signal discussed in this work was investigated for a probe pulse delayed from the pump pulse by more than 0.5 ns, in order to give enough time for the photoexcited electron-hole pairs to recombine.[16] The measured TRE signal then is solely due to electrons that permanently reside in the dots.

Although the investigated structure has an average occupation of one electron per dot, it also contains small amounts of undoped dots, as well as multiply negatively charged dots. For the undoped structures exciton spin coherence gives only negligible contributions after 0.5-ns delay. For the second

type there is no contribution from ground-state electron spin coherence, while there could be excited-state contributions. However, when scanning the pump laser across the p shell the spectral dispersion (see below) does not show the behavior that would be expected if there were a significant fraction of such structures.

We also note that the optical pump excitation does not cause charge accumulation in the QDs: first, the excitation occurs below barrier; second, for charged dots there is no dark ground-state exciton configuration. In addition, when monitoring the photoluminescence emission under the excitation conditions used for the ellipticity studies we do not observe significant excited-state emission. Thus we conclude that the TRE signal shown in Fig. 2 must be associated with QDs containing a single resident electron.

The TRE signal was Fourier analyzed, and the Fourier transforms are shown in Fig. 2(b). The position of each the peak in the Fourier spectrum equals the Larmor precession frequency, ω_L, associated with a given oscillatory component in the TRE signal. Every Larmor frequency can be translated into the absolute value of the g factor of the precessing electrons that give rise to the associated TRE oscillation, through

$$|g| = \frac{2m}{eB}\omega_L, \tag{1}$$

where m is the free electron mass, e is the elementary charge, and B is the applied magnetic field strength.

The g factor obtained from (1) is plotted as a function of the excitation energy in Fig. 1. At low energies (below 1.40 eV), a single g factor characterizes the TRE signal, in agreement with previous measurements of time-resolved pump-probe Faraday rotation (TRFR) on this same sample.[24,27] The observation of a single g factor for excitation below 1.40 eV is well understood, and it is associated with electrons belonging to a subset from the QD ensemble, where the energy for creation of a trion in the ground-state s shell matches the range of photon energies contained in the exciting laser pulse.[16] The smooth change with optical transition energy shows that the g-factor variation across the ensemble emission is mostly determined by the band-gap energy.

However, for pump photon energies in the range of 1.40–1.45 eV, the TRE signal contains two Fourier frequencies, and, therefore, two groups of electrons, of differing g factors, must be contributing to the TRE signal. From a comparison with the emission spectrum it is noticeable that the second g factor appears when the pumping photon energy is resonant with the high energy tail of the PL band, i.e., when the excitation approaches resonance with excited QD states. Figure 1 shows also that the g-factor branch that appears starting at an excitation energy of 1.40 eV repeats the same values of the g-factor branch that emerges at excitation photon energies starting at 1.36 eV. This result is suggestive that spin coherence in a given quantum dot can be once again generated when the pumping energy is increased by about 40 meV.

In order to understand how an electron in a given QD can be spin oriented at two very different excitation energies, we shall examine the excitation spectrum for a negatively charged dot,[28] shown in Fig. 3. The ground state, e_s, of the QD is given by a resident electron in the s shell. The lowest energy trion

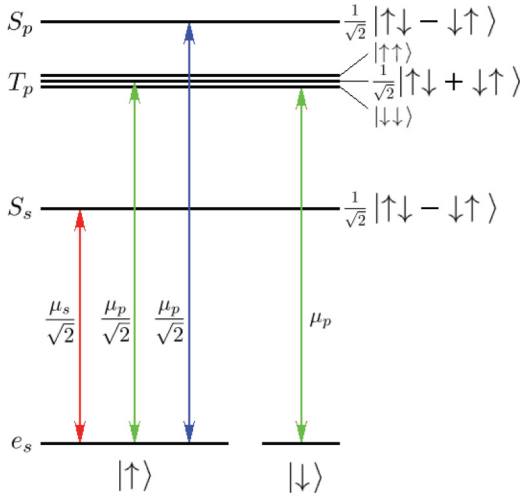

FIG. 3. (Color online) Scheme of the energy hierarchy of the trions (S_s, T_p, and S_p) that can be photoexcited in a charged QD through tuning the pump laser in resonance with s- and p-shell transitions, measured from the ground state e_s. The splitting between the T_p and S_s state is deduced from the TRE spectra to be 40 meV. The arrows show the coupling, by right-hand circularly polarized light, of the ground state—consisting of a dot containing an electron whose spin function has a spin-up component (left) and spin-down component (right)—to the excited states, whereby the QD contains a trion. The spin function of the electrons associated with the trion states are shown in the right column. The allowed transitions and the corresponding oscillator strengths are shown.

that can be photoexcited is composed of an additional electron in the same s shell, but with spin opposite to that of the first electron, plus a hole in a valence s shell. We shall denote this trion as S_s, to symbolize the electronic spin of zero representing a singlet, and the subscript to symbolize the s-shell character of the photoexcited particles. In the next optically allowed trion state, the photoexcited electron and hole will be excited in their respective p shells; such a trion can be excited with a total electronic spin of zero or unity, representing a singlet (S_p) or a triplet (T_p), respectively. Excitation thus offers some flexibility with respect to the polarization of the exciting laser, as the Pauli exclusion principle is not effective in the excitation process.

The triplet state T_p is lower in energy than the singlet S_p by a few meV,[29–31] due to the electron-electron exchange interaction, Δ_{ee}. The T_p state has an inner fine structure, due to the electron-hole exchange interaction, but we will ignore it in the following because the splitting is much smaller than Δ_{ee}.

The emergence of a second g factor for an excitation photon of energy higher than 1.40 eV can be understood if we notice that for excitation in this energy range two different subsets of the QD ensemble are simultaneously excited, as shown in Fig. 4. In one subset, the excitation light creates S_s trions directly, whereas in the other subset T_p or S_p trions are created, which is followed by energy relaxation into the trion ground state S_s. A trion may relax energy by a combination of Auger or phonon relaxation for the electron and acoustic phonon emission for the hole, in a time scale of tens of picoseconds.[32,33] Differential transmission measurements

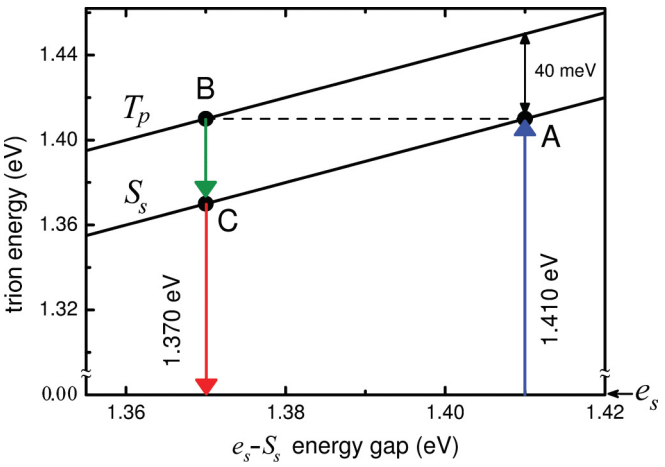

FIG. 4. (Color online) Energy of the S_s and T_p trion states as a function of the energy gap e_s-S_s of the QD ensemble in the sample investigated. Photons of 1.410-eV energy are able to simultaneously excite two subsets of the QD ensemble: a subset at A into the S_s trion state and another subset at B into the T_p trion state.

mapping the s-shell population as a function of time after the arrival of an excitation pulse resonant with the p-shell estimate the characteristic intershell relaxation time to be 20–30 ps.[26]

Let us consider now the generation of spin coherence by the exciting light pulse in more detail. We note that the underlying physics is closely related to the effect of negative circular polarization observed in the QD photoluminescence of singly negatively charged QDs (see, for example, Ref. 34): nonresonant circular polarized excitation, either into excited dot shells or even into the wetting layer, leads dominantly to ground state emission of opposite circular polarization. As a consequence, the electron left behind after recombination has the same spin orientation as the optically injected one. To explain how this process occurs, the exchange interactions need to be included in the considerations. In our studies, in addition a transverse magnetic field is applied, and the resulting spin precession is an important aspect for the spin initialization and accumulation, which leads to 100% electron spin polarization in the photoexcited QD ensemble after a sufficiently long laser pulse train.

The generation of spin coherence by an incoming light pulse in a QD containing a resident electron has been described in Ref. 35. Generally, the initial state of an electron resident in a QD is a superposition state of a spin-up component, which we shall denote by $|\uparrow\rangle$, and a spin-down component, which we shall denote by $|\downarrow\rangle$, where the quantization axis is taken along the light wave vector. If a quantizing magnetic field, $\boldsymbol{B}$, is applied in the Voigt geometry, then the equilibrium spins will align themselves parallel, or antiparallel, to $\boldsymbol{B}$, in which case the spin wave function of a resident electron can be written as $\frac{1}{\sqrt{2}}|\uparrow \pm \downarrow\rangle$.[36] Let us consider a right-hand circularly polarized photon, denoted σ^+, resonant with the $e_s \rightarrow S_s$ transition. According to well-known optical selection rules for III-V materials, a σ^+ laser pulse photogenerates an electron-hole pair, in which the electron has spin down, and occupies the same orbital state as the resident electron.

Therefore, because of Pauli exclusion principle, the σ^+ pulse can only excite the $|\uparrow\rangle$ component of the initial electron state. The spin function associated with a photogenerated trion in the singlet S_s state is $\frac{1}{\sqrt{2}}|\uparrow\downarrow - \downarrow\uparrow\rangle$. This excitation process is shown by the leftmost arrow in Fig. 3. The exciting pump laser drives the electron into a superposition state of electron and trion. The electrons in the trion are not precessing as the electron-electron exchange pushes them into a singlet state with spin zero. Because of the applied Voigt magnetic field, the hole in the trion component of the superposition state precesses during the trion lifetime of 400 ps[16] and can recombine with any of the two electrons in the singlet trion. Therefore, the electronic spin component which was excited (in this case $|\uparrow\rangle$) becomes in effect randomized after recombination, while the nonexcited original electron spin component (in this case $|\downarrow\rangle$) gets pumped and accumulates from pulse to pulse to give the TRE signal that we detect after trion recombination. Notice that to verify which spin function component of the resident electron, $|\uparrow\rangle$ or $|\downarrow\rangle$, can be excited by a σ^+ pulse, it is sufficient to inspect the projection of the electronic spin function of the trion on $|\uparrow\downarrow\rangle$ or $|\downarrow\downarrow\rangle$, respectively, the result being shown in Fig. 3.

The analysis for the TRE signal when pumping at the $e_s \rightarrow S_s$ transition can be extended to the $e_s \rightarrow T_p$ and $e_s \rightarrow S_p$ transitions, where one electron is in the s shell, while the other one is in the p shell. The T_p triplet state is associated with three different electronic spin functions, that correspond to a total spin projection of -1, 0, or $+1$ on the excitation light wave vector. The electronic spin functions associated with the T_p and S_p trion states are shown in Fig. 3. Note that the different triplet trion states are coupled by the transverse magnetic field, which is, however, weaker than the effects of the electron-electron exchange.

In creating a T_p or S_p trion, circularly polarized light again excites only a particular spin component of the spin function of the electron in the initial state. Any unexcited electron spin component, because of selection rule and/or insufficient pump power, is, therefore, accumulated by the periodic sequence of excitation pulses. For example, a σ^+-polarized pulse creates an electron-hole pair in which the photogenerated electron is in a $|\downarrow\rangle$ spin state. If a σ^+ pulse is resonant with the S_p state, then only the $|\uparrow\rangle$ spin component of the resident electron can be excited, as indicated by the third arrow from the left in Fig. 3. After orbital relaxation and recombination of the trion, the electron spin component $|\uparrow\rangle$ of the resident electron is randomized, while the nonexcited component $|\downarrow\rangle$ gets amplified.

On the other hand, for a σ^+ pulse of appropriate photon energy, T_p can be excited through both the $|\downarrow\rangle$ and $|\uparrow\rangle$ components of the spin function of the resident electron (indicated by the second and fourth arrows from the left, respectively, in Fig. 3). The first one results in a spin triplet with -1 projection on the optical axis, and the second one in a triplet with 0 projection. These transitions, however, are described by different oscillator strengths, as indicated in Fig. 3. As a consequence, a net spin pumping can occur, since the two initial electron spin components are converted fully into trion states (requiring π-pulse power area) for different pump pulse areas. The amplitude and phase of the spin coherence that is reached in the end are the result of a complex process involving

carrier relaxation into the ground state, carrier spin precession, and radiative recombination.

In Ref. 28 a π-phase shift between pumping the excited singlet and triplet trions S_p and T_p was predicted but could not be observed. This phase shift can be understood in the following way, neglecting for simplicity the hole spin precession because of its small in-plane g factor. When resonant with the $e_s \rightarrow T_p$ transition, due to the dipole moment coupling of $|\downarrow\rangle$ to T_p being greater than the one coupling $|\uparrow\rangle$ to T_p, a σ^+ pulse arriving at $t = 0$ photoexcites predominantly the $|\downarrow\rangle$ component of the spin function of the resident electron. Hence, the nonexcited component $|\uparrow\rangle$ accumulates. Therefore, the TRE signal coming from $e_s \rightarrow T_p$ excitation will be dominated by the time evolution of the $t = 0$ spin-up component of the spin function of the resident electron. In contrast, as described above, an $e_s \rightarrow S_p$ excitation pumps and accumulates the spin-down component of the spin function of the resident electron, which evolves in time in phase opposition to the spin-up component.

This phase change was tested by extracting the phase, φ, from the experimental TRE oscillations, fitting each spin precession component with the function $A\, e^{-t/\tau} \cos(\omega t + \varphi)$,[24] whereby ω was fixed at the value Larmor precession frequency, $\omega = \omega_L$, extracted from the Fourier transform [see Fig. 2(b)]. Figure 5(a) shows the amplitude, A, and phase, φ, of the TRE signal obtained in that way, as a function of the excitation photon energy. The amplitude across the s shell reproduces quite well the PL line shape of the QD ensemble shown in Fig. 1, demonstrating that the same QDs are responsible for the PL and TRE signals. When moving into the p shell, the greatest amplitude achieved for the p-pumped TRE oscillations is about five times smaller than that of the greatest amplitude from s-pumped QDs. This is partly explained by the fact that, in the former case, the probe beam is off-resonance with the tested spin-polarized electrons in the s shell by the thereby estimated s-p shell splitting of 40 meV, whereas, in the latter case, the probe beam is resonant. The ellipticity signal intensity is maximum for resonant conditions and drops continuously with increasing separation between probe photon energy and probed resonance energy.[37]

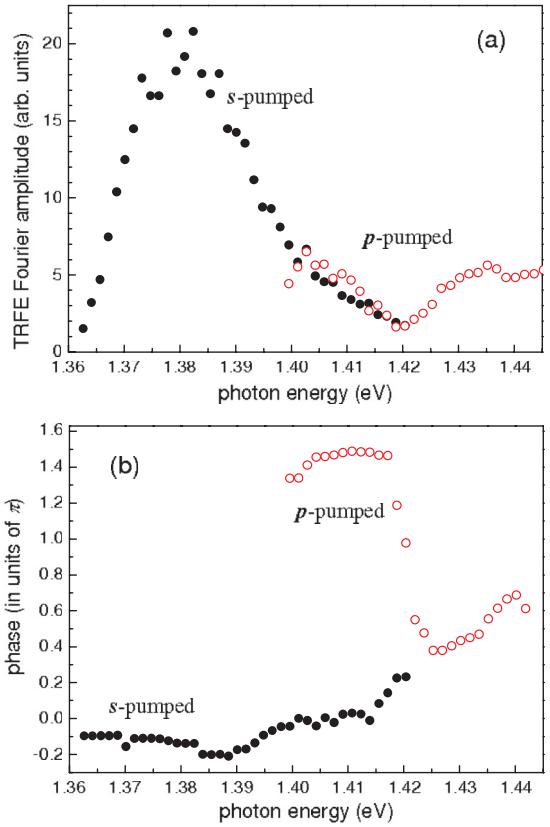

FIG. 5. (Color online) (a) Amplitude and (b) phase of the TRE oscillatory components as a function of excitation energy.

However, the behavior is more involved: The amplitude of the ellipticity signal in Fig. 5(a) does not drop continuously when moving the probe energy across the p shell to higher values, but it instead shows a maximum on the high energy flank of the s shell, and a dip at about 1.42 eV, followed by another maximum. This can be understood in the following way. The pump and probe contain photons with an energy width of about 2 meV, which is smaller than the expected splitting between S_p and T_p.[30] So in a given dot we may excite one of these two states, but not both. However, in the inhomogeneous ensemble, in a fraction of dots we excite T_p trions, while in another fraction S_p is excited. According to previous consideration, the resident electron spin polarization in these two fractions have opposite orientations, which further reduces the absolute value of the ellipticity signal as compared to s-shell excitation.

Due to the smaller energy of T_p as compared to S_p, for pump energies resonant with the low energy flank of the p shell (coinciding with the high energy flank of the s shell) the signal of the electrons from T_p excitation will dominate. When the pump-probe energy reaches the p-shell center, the spin coherence contributions from T_p and S_p excitation roughly compensate each other, resulting in the dip in the signal. Moving across the p-shell maximum, the spin coherence from S_p excitation dominates resulting in the revival of the p-pumped ellipticity signal seen on the high-energy side in Fig. 5. If this interpretation is correct, then the predicted π shift of the ellipticity signal should occur across the amplitude minimum.

The phase of the TRE signal is shown in Fig. 5(b) and follows these predictions quite well: when moving across the p shell the phase drops by about π from almost 1.5π to about 0.4π over an energy range that conincides with the energy range of the minimum ellipticity amplitude. This confirms that, indeed, mostly the $|\downarrow\rangle$ component of the resident electron spin is excited when the pump photon energy is in resonance with the T_p trion transition, leading to the observed π phase shift, and can be explained by the larger dipole moment coupling of the $|\downarrow\rangle$ spin component to T_p than the $|\uparrow\rangle$ coupling to T_p, as indicated in Fig. 3.

The full width of the range over which this phase shift occurs is 7 meV, and we might take the half width (3.5 meV) as an estimate of the splitting between the S_p and T_p configurations, which is a measure of the electron-electron exchange energy, Δ_{ee}. This value pretty much coincides with the small kink in the energy dispersion of the larger valued g factors (the red symbols in Fig. 2) observed around 1.42 eV. If one extrapolates the values below and above this energy by linear dependencies to lower and higher energies one finds also a horizontal

energy shift between the two linear dependencies to be 3 to 4 meV.

Surprisingly, when one moves the pump-probe energy from the p shell into the s shell a phase shift by 1.5 π occurs compared to T_p excitation, and about 0.4 π compared to S_p excitation. Our considerations so far predicted, for example, no phase difference between the spin coherence generated with S_s or S_p excitations. However, thus far the finite relaxation time from p to s shell was not taken into account. For nonresonant excitation the randomization of the optically excited ground-state electron spin component can start only after relaxation into the ground state, whereas for direct s-shell excitation the generation may start immediately after the pump pulse hits the sample at time zero. Time-resolved differential transmission measurements[26] monitoring the S_s population after the arrival of the pump pulse confirm that for resonant excitation the S_s population increases immediately, whereas for pumping the T_p state the S_s population increase is delayed by the $T_p \rightarrow S_s$ relaxation time, estimated at 20–30 ps. Therefore, for p-shell excitation time zero is, in effect, shifted by the relaxation time: The unexcited electron spin component precesses until relaxation of the excited trion component into the S_s has occurred. The moment right after relaxation is equivalent to a direct S_s excitation, except that the phase of the unexcited component $|\downarrow\rangle$ has altered correspondingly because of the spin precession. This time shift has to be compared to the spin precession period, which for the electron g factors measured in Fig. 1 ranges from 90 to 100 ps. The time shift by a 25-ps relaxation time (roughly 25% of the precession period) leads to a phase shift by about 0.5 π, in approximate agreement with Fig. 6 when comparing the cases of S_s and S_p excitation. The change in the phase when varying the photon energy around resonance with S_p excitation might reflect variations of the relaxation time.

We also observe that when a trion is excited into a T_p state, its relaxation into an S_s involves the relaxation of an electron from the p shell into the s shell, in which the spin-parity of the electrons in the trion changes from triplet to singlet; therefore, in the $T_p \rightarrow S_s$ relaxation, an electron spin-flip is required. The spin degrees have so far mostly been neglected in works addressing carrier spin relaxation. However, also for doped QDs fast carrier relaxation has been observed,[26] which is not hampered by the Pauli principle. This suggests that the phonon emission which is energetically required for relaxation can be accompanied by a proper electron spin-flip to make the relaxation possible. In Ref. 30 it was shown that such spin-flip processes may be facilitated by the asymmetric electron-electron exchange interaction.

IV. CONCLUSIONS

In conclusion, we have demonstrated that spin coherence can be generated in an ensemble of negatively charged self-assembled QDs by pumping the excited trion states. Nonresonant spin initialization is of interest, as it contributes, e.g., to suppressing stray light troublesome in resonant measurements. When sweeping the energy of the pump photons in a 7 meV interval, the phase of the induced spin coherence can be changed by π. This effect could be exploited for phase inversion in the initialization step. We also note that we have obtained through these spin coherent measurements data on the QDs, such as estimates for the splitting between the p and s shells, and for the splitting between excited triplet and singlet states, which cannot be accessed through linear spectroscopy because of the strong inhomogeneities in the ensemble.

ACKNOWLEDGMENTS

A.B.H. acknowledges financial support provided by CNPq (Projects 500660/2011-5, 304685/2010-0 and 475296/2009-5), FAPESP (Project 2010/10452-8), LNLS-Brazilian Synchrotron Light Laboratory/MCT (LMF), and thanks P. M. Koenraad for profitable discussions. M.B. acknowledges the support of the Deutsche Forschungsgemeinschaft (BA1549/11-3).

[1] F. Meier and B. P. Zakharchenya, eds., *Optical Orientation* (North-Holland, Amsterdam, 1984).

[2] M. Kroutvar, Y. Ducommun, D. Heiss, M. Bichler, D. Schuh, G. Abstreiter, and J. Finley, Nature **432**, 81 (2004).

[3] M. V. G. Dutt, J. Cheng, B. Li, X. Xu, X. Li, P. R. Berman, D. G. Steel, A. S. Bracker, D. Gammon, S. E. Economou, Ren-Bao Liu, and L. J. Sham *et al.*, Phys. Rev. Lett. **94**, 227403 (2005).

[4] M. Atatüre, J. Dreiser, A. Badolato, A. Högele, K. Karrai, and A. Imamoglu, Science **312**, 551 (2006).

[5] X. Xu, Y. Wu, B. Sun, Q. Huang, J. Cheng, D. G. Steel, A. S. Bracker, D. Gammon, C. Emary, and L. J. Sham, Phys. Rev. Lett. **99**, 097401 (2007).

[6] A. J. Ramsay, S. J. Boyle, R. S. Kolodka, J. B. B. Oliveira, J. Skiba-Szymanska, H. Y. Liu, M. Hopkinson, A. M. Fox, and M. S. Skolnick, Phys. Rev. Lett. **100**, 197401 (2008).

[7] D. Press, K. D. Greve, P. L. McMahon, T. D. Ladd, B. Friess, C. Schneider, M. Kamp, S. Hofling, A. Forchel, and Y. Yamamoto, Nat. Photon. **4**, 367 (2010).

[8] K. C. Nowack, F. H. L. Koppens, Y. V. Nazarov, and L. Vandersypen, Science **318**, 1430 (2007).

[9] Y. Wu, E. D. Kim, X. Xu, J. Cheng, D. G. Steel, A. S. Bracker, D. Gammon, S. E. Economou, and L. J. Sham, Phys. Rev. Lett. **99**, 097402 (2007).

[10] D. P. D, T. H. Ladd, B. Zhang, and Y. Yamamoto, Nature **456**, 218 (2008).

[11] C. Phelps, T. Sweeney, R. T. Cox, and H. Wang, Phys. Rev. Lett. **102**, 237402 (2009).

[12] G. D. Fuchs, V. V. D. D. M. Toyli, F. J. Heremans, and D. Awschalom, Science **326**, 1520 (2009).

[13] E. D. Kim, K. Truex, X. Xu, B. Sun, D. G. Steel, A. S. Bracker, D. Gammon, and L. J. Sham, Phys. Rev. Lett. **104**, 167401 (2010).

[14] D. Loss and D. P. DiVincenzo, Phys. Rev. A **57**, 120 (1998).

[15] G. Slavcheva and P. Roussignol, eds., *Optical Generation and Control of Quantum Coherence in Semiconductor Nanostructures* (Springer-Verlag, Berlin, 2010).

[16] A. Greilich, R. Oulton, E. A. Zhukov, I. A. Yugova, D. R. Yakovlev, M. Bayer, A. Shabaev, A. L. Efros, I. A. Merkulov, V. Stavarache, D. Reuter, and A. Wieck, Phys. Rev. Lett. **96**, 227401 (2006).

[17] I. Zutic, J. Fabian, and S. D. Sarma, Rev. Mod. Phys. **76**, 323 (2004).

[18]M. Wu, J. Jiang, and M. Weng, Phys. Rep. **493**, 61 (2010).
[19]A. Greilich, D. R. Yakovlev, A. Shabaev, A. L. Efros, I. A. Yugova, R. Oulton, V. Stavarache, D. Reuter, A. Wieck, and M. Bayer, Science **313**, 341 (2006).
[20]P. E. Hohage, G. Bacher, D. Reuter, and A. D. Wieck, Appl. Phys. Lett. **89**, 231101 (2006).
[21]A. Greilich, S. E. Economou, S. Spatzek, D. R. Yakovlev, D. Reuter, A. D. Wieck, T. L. Reinecke, and M. Bayer, Nat. Phys. **5**, 262 (2009).
[22]H. S. Nguyen, G. Sallen, C. Voisin, P. Roussignol, C. Diederichs, and G. Cassabois, Phys. Rev. Lett. **108**, 057401 (2012).
[23]S. A. Crooker, D. D. Awschalom, and N. Samarth, IEEE J. Sel. Top. Quantum Electron. **1**, 1082 (1995).
[24]A. Schwan, B.-M. Meiners, A. B. Henriques, A. D. B. Maia, A. A. Quivy, S. Spatzek, S. Varwig, D. R. Yakovlev, and M. Bayer, Appl. Phys. Lett. **98**, 233102 (2011).
[25]A. Shabaev, E. A. Stinaff, A. S. Bracker, D. Gammon, A. L. Efros, V. L. Korenev, and I. Merkulov, Phys. Rev. B **79**, 035322 (2009).
[26]H. Kurtze, J. Seebeck, P. Gartner, D. R. Yakovlev, D. Reuter, A. D. Wieck, M. Bayer, and F. Jahnke, Phys. Rev. B **80**, 235319 (2009).
[27]A. Schwan, B.-M. Meiners, A. Greilich, D. R. Yakovlev, M. Bayer, A. D. B. Maia, A. A. Quivy, and A. B. Henriques, Appl. Phys. Lett. **99**, 221914 (2011).
[28]S. G. Carter, S. C. Badescu, and A. S. Bracker, Phys. Rev. B **81**, 045305 (2010).
[29]R. J. Warburton, C. Schaflein, D. Haft, F. Bickel, A. Lorke, K. Karrai, J. M. Garcia, W. Schoenfeld, and P. M. Petroff, Nature **405**, 926 (2000).
[30]M. E. Ware, E. A. Stinaff, D. Gammon, M. F. Doty, A. S. Bracker, D. Gershoni, V. L. Korenev, S. C. Badescu, Y. Lyanda-Geller, and T. L. Reinecke, Phys. Rev. Lett. **95**, 177403 (2005).
[31]A. Schwan, S. Varwig, A. Greilich, D. R. Yakovlev, D. Reuter, A. D. Wieck, and M. Bayer, Appl. Phys. Lett. **100**, 232107 (2012).
[32]T. S. Sosnowski, T. B. Norris, H. Jiang, J. Singh, K. Kamath, and P. Bhattacharya, Phys. Rev. B **57**, R9423 (1998).
[33]G. A. Narvaez, G. Bester, and A. Zunger, Phys. Rev. B **74**, 075403 (2006).
[34]S. Cortez, O. Krebs, S. Laurent, M. Senes, X. Marie, P. Voisin, R. Ferreira, G. Bastard, J. M. Gerard, and T. Amand, Phys. Rev. Lett. **89**, 207401 (2002).
[35]A. Greilich, D. R. Yakovlev, and M. Bayer, in *Optical Generation and Control of Quantum Coherence in Semiconductor Nanostructures*, edited by G. Slavcheva and P. Roussignol (Springer-Verlag, Berlin, 2010).
[36]L. D. Landau and E. M. Lifshitz, *Quantum Mechanics, Non-Relativistic Theory,* Course of Theoretical Physics, Vol. 3 (Addison-Wesley, Reading, MA, 1965).
[37]M. M. Glazov, I. A. Yugova, S. Spatzek, A. Schwan, S. Varwig, D. R. Yakovlev, D. Reuter, A. D. Wieck, and M. Bayer, Phys. Rev. B **82**, 155325 (2010).